Supporting Information

Trace Ammonia Removal from Air by Selective Adsorbents Reusable with Water

Akira Takahashi*[1], Kimitaka Minami[1], Keiko Noda[1], Koji Sakurai[1], and Tohru Kawamoto*[1]

Nanomaterials Research Institute, National Institute of Advanced Industrial Science and Technology (AIST), 1-1-1 Higashi, Tsukuba 305-8565, Japan[1]

Author information

Corresponding author

Akira Takahashi* email: akira-takahashi@aist.go.jp

Tohru Kawamoto* email: tohru.kawamoto@aist.go.jp

Table of contents

1. Conditions of the tests

The conditions of tests throughout main manuscript and SI are summarized briefly in table S1.

Table S1 Conditions of tests

stage	Number of PBAs	Purpose	Methods
First screening	70	Screening of adsorption capacity with FTIR	The height of ammonium peak in PBAs of around 1400 cm^{-1} was evaluated after adsorbing ammonia at 10 ppbv. The details are described in part 1 in SI.
Second screening	12	Screening of desorption capacity with acid washing and evaluation of stability with PXRD and FTIR	PBAs of absorbing ammonia gas (final concentration was 200 ppmv) in humid air were washed with 1 mol/L of sulfuric acid. The PXRD patterns and FTIR spectra of initial, after adsorption, after desorption of PBAs were evaluated. The details are described in part 2 in SI.
Adsorption with trace ammonia	7	Evaluation of adsorption capacity in trace ammonia	The adsorption capacities in 10 ppmv of ammonia were evaluated with column test. The details are described in methods of main manuscript
Recovery with water flushing	3 (PB, CuPBA, CoPBA)	Evaluation of desorption capacity with water flushing	The recovery of adsorbed ammonia was evaluated with water flushing. The details are described in methods of main manuscript.
Cyclic test	1, CoPBA	Evaluation of cyclic adsorption and desorption	The cyclic adsorption and desorption with water flushing test was performed for 10 times. The details are described in methods of the main manuscript.
Adsorption in livestock farm	1, CoPBA	Evaluation of PBA as reusable ammonia adsorbent in actual condition	Ammonia adsorption and recovery of the PBA in actual humid air from a livestock farm was evaluated. The details are described in methods of the main manuscript.

2. First screening test of Prussian blue analogues for ammonia adsorbents

Firstly, a survey test for ammonia adsorption capacity of 70 Prussian blue analogues (PBAs) was performed. The thin film of Prussian blue analogues on ITO substrate set in room air containing about 10 ppbv of ammonia were used for the evaluation, because it was revealed in a previous study that thin films of PBAs perform as adsorbent from a low concentration of approximately 10 ppbv. The amount of ammonia in PBAs was evaluated by means of a Fourier transform infrared spectrometer (FTIR, Nicolet iS5 Thermo Fisher Scientific Inc.) and a diamond ATR apparatus. As a result, 10 PBAs indicating higher peak of N-H bending at 1400 cm^{-1} were selected

3. Second screening test of Prussian blue analogues for ammonia adsorbent

Following the first screening test, 10 kinds of Prussian blue analogues ($M^{\alpha+}[M'^{\beta+}(CN)_6]_{1-x}$) with different combination of M^{2+} and $M'^{\beta+}$ metals were selected. Hereafter, materials with chemical compositions of $M^{2+}[M'^{\beta+}(CN)_6]_{1-x}$ as MPBA($M'^{\beta+}$) were described except for PB, CuPBA and CoPBA described in main manuscript. CuPBA, MnPBA(Fe^{II}), ZnPBA(Fe^{II}), NiPBA(Fe^{II}), CuPBA(Fe^{III}), ZnPBA(Fe^{II}), NiPBA(Fe^{II}), CoPBA, MnPBA(Mn^{III}), ZnPBA(Fe^{III}) were synthesized by mixing 0.6 mol/L of $M^{2+}A$(A means anion as following, Cl_2 for Co^{2+}, SO_4 for Cu^{2+}, Zn^{2+} and Fe^{2+}, and $(NO_3)_2$ for Mn^{2+} and Ni^{2+}) in aqueous solution and 0.2 mol/L of $K_{(6-\beta)}[M'^{\beta+}(CN)_6]$ in aqueous solution for 1 night at 50 ˚C, 1000 rpm using SI-300C. The precipitations were then washed with ultrapure water 6 times and dried in a vacuum.

A batch adsorption test for these 12 PBAs (including the previous 10 and Prussian blue (PB) and potassium copper Prussian blue ($K_2Cu_3[Fe(CN)_6]_2$, KCuPBA(Fe^{II})) obtained from Kanto chemical) was performed. Each 50 mg of samples were set on a watch glass and left in a desiccator containing 50 mL of 0.28 wt% ammonia water in a beaker for 3 days, so that the samples would be exposed to ammonia vapor released by the ammonia water. At the end of adsorption test, the concentration of ammonia was 200 ppmv, evaluated by an ammonia detection tube (3M, GASTEC Corp.).

Following the batch adsorption test, desorption amount of ammonia was evaluated by washing with 1 mol/L sulfuric acid. 10 mg of ammonia adsorbing sample was put into a 15 mL centrifuge tube containing 10 mL of 1 mol/L sulfuric acid. The tubes were shaken using SI-300 at 25 ˚C, 600 rpm for 1 night. After shaking, the solutions were filtered with 0.45 μm paper filters. The concentrations of the ammonium cation in the so obtained solutions were evaluated by means of ion-chromatography (IC-883, Metrhom).

The solution of ZnPBA(Fe^{III}) appeared light yellow in colour, indicating the decomposition of ZnPBA(Fe^{III}) after the adsorption of ammonia. The solids obtained from the filters were dried at 60 ˚C. The desorbed amounts of

ammonium cation are shown in Fig. S1. Mn PBA(Fe^{II}) yielded no solids after desorption, due to complete dissolution in the solution.

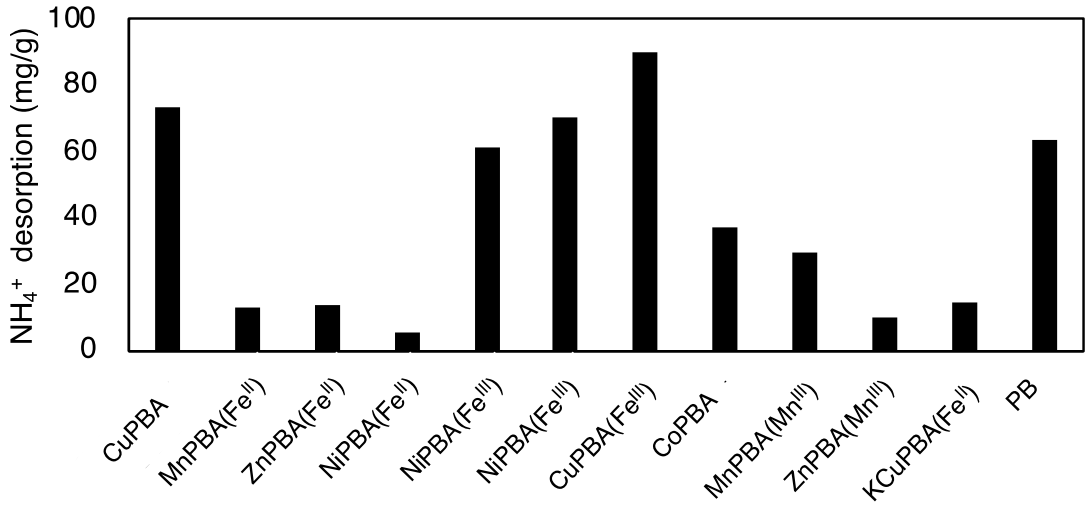

Figure S1. Desorption amount of ammonium cation from PBAs adsorbing ammonia

In order to evaluate the stability of PBAs through the ammonia adsorption and desorption processes, PXRD patterns were measured, and FTIR spectra of PBAs in initial, after batch adsorption, after desorption with 1 mol/L of sulfuric solution were obtained. The PXRD patterns in Fig. S2 and S3 show that CuPBA, Zn PBA(Fe^{II}), Ni PBA(Fe^{II}), Ni PBA(Fe^{III}), Co PBA, PB, and KCuPBA(Fe^{II}) retained their crystal structure in each of the conditions. The FTIR spectra in Fig S4, S5 show that CuPBA, ZnPBA(Fe^{II}), CoPBA, PB, and KCuPBA(Fe^{II}) feature no CN peak shift stretching around 2100 cm^{-1}, indicating that no structure change occurred during the adsorption/desorption processes.

In conclusion, showing the highest ammonia adsorption capacity and stability, CuPBA, CoPBA, and PB were selected as most suitable ammonia adsorbents for the experiment.

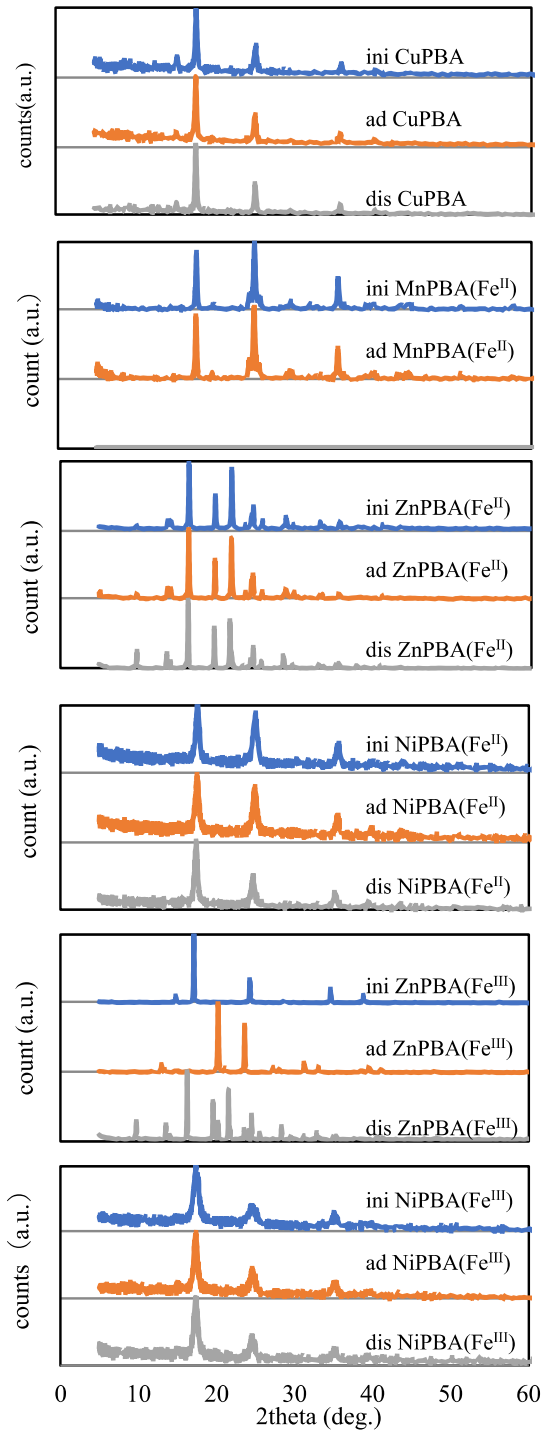

Figure S2. PXRD pattern of CuPBA, Mn PBA(Fe^{II}), Zn PBA(Fe^{II}), Ni PBA(Fe^{II}), Zn PBA(Fe^{III}), and NiPBA(Fe^{III}) . The prefixes “ini”, “ad”, and “des” indicate initial, after adsorbing ammonia, and after desorbing ammonia, respectively.

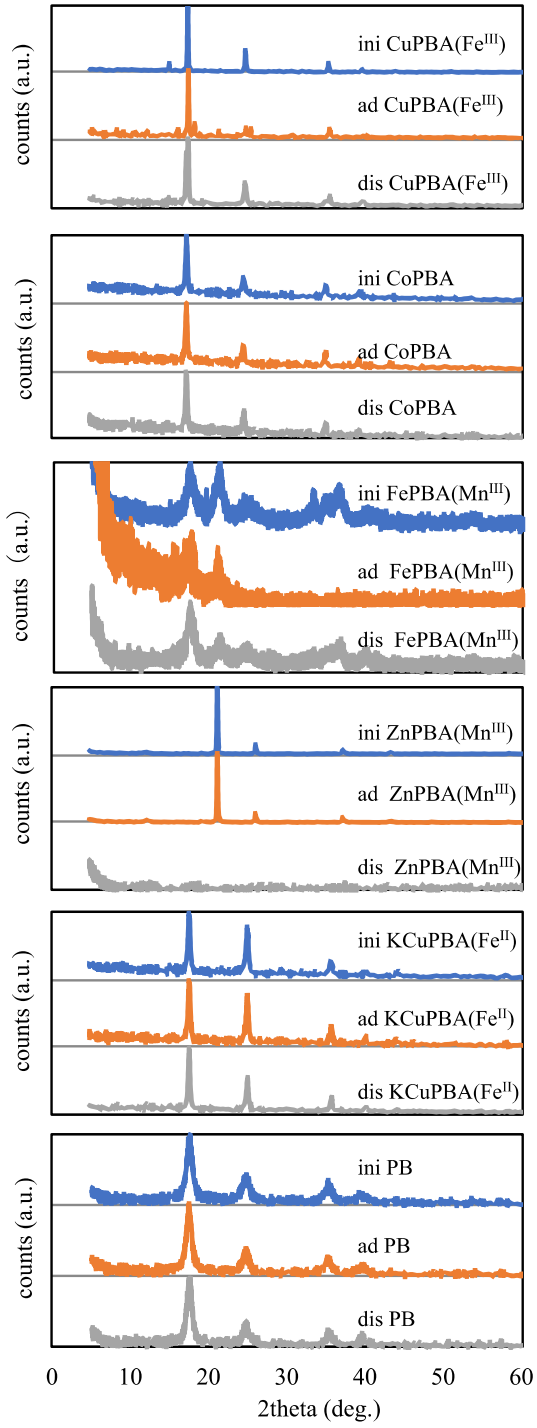

Figure S3. PXRD pattern of CuPBA(Fe^{III}), CoPBA, FePBA(Mn^{III}), ZnPBA(Mn^{III}), KCuPBA(Fe^{II}), and PB. The prefixes “ini”, “ad”, and “des” indicate initial, after adsorbing ammonia, and after desorbing ammonia, respectively.

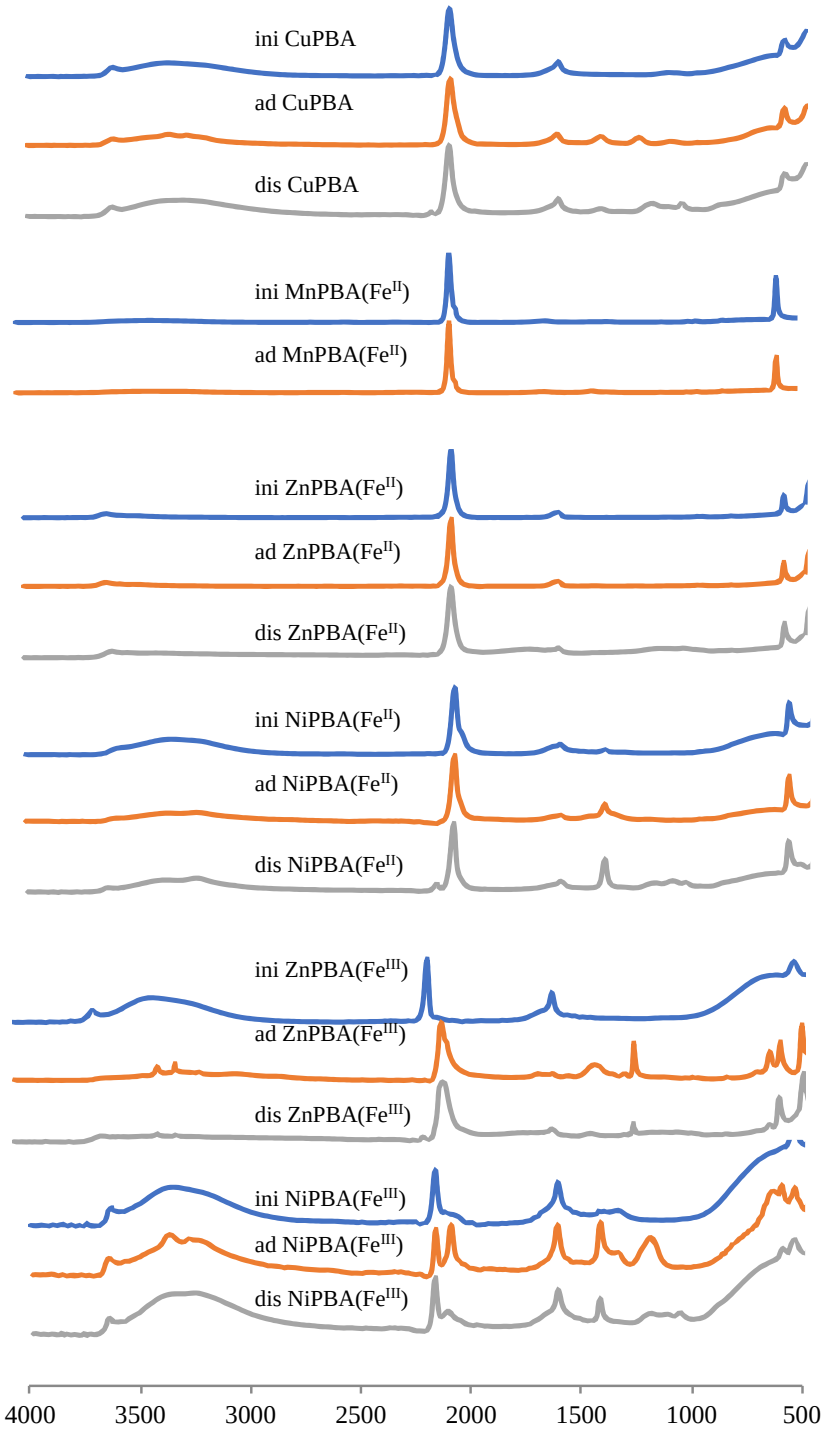

Figure S4. FTIR spectrum of CuPBA, MnPBA(Fe^{II}), ZnPBA(Fe^{II}), NiPBA(Fe^{II}), CuPBA(Fe^{III}), ZnPBA(Fe^{III}), and NiPBA(Fe^{III}). The prefix ini, ad, and des represent the initial state, after adsorbing ammonia, and after desorbing ammonia, respectively.

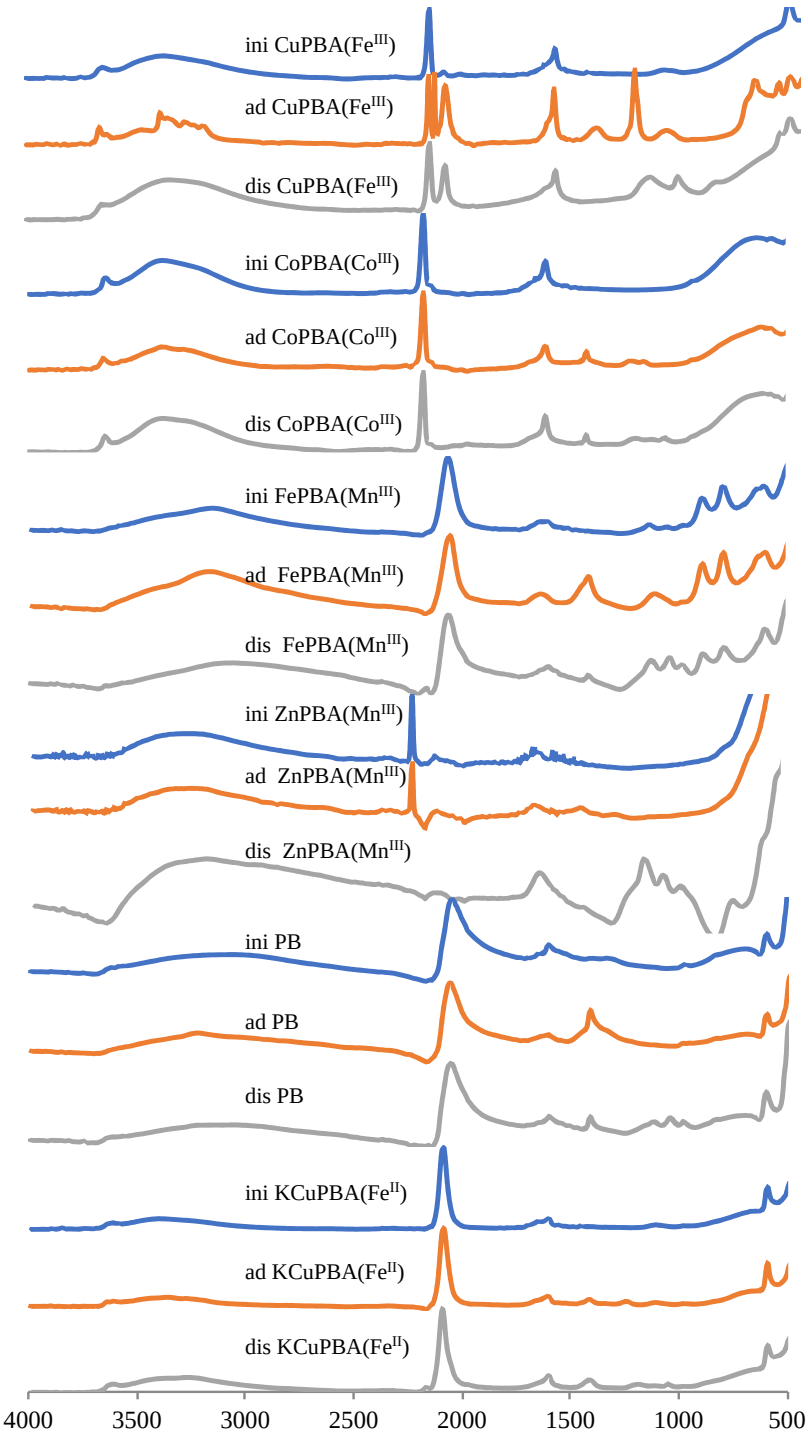

Figure S5 FTIR spectrum of CuPBA(Fe^{III}), CoPBA, FePBA(Mn^{III}), ZnPBA(Mn^{III}), PB, and KCuPBA(Fe^{II}). The prefixes “ini”, “ad”, and “des” indicate the initial state, after adsorbing ammonia, and after desorbing ammonia, respectively.

4. column adsorption test

The schematic figure of column adsorption apparatus was described in Fig. S6. The results of PBA were shown in Table S2.

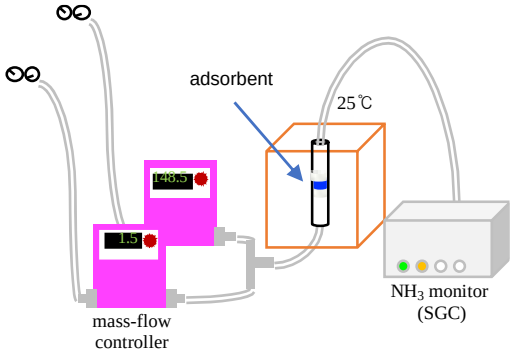

Figure S6 Schematic figure of column adsorption test

Table S2 ammonia adsorption capacity of PBAs at 10 ppmv

sample	composition of PBA	capacity (mmol/g)
PB	$Na_{0.05}Fe[Fe(CN)_6]_{0.70}\cdot 5.3H_2O$	3.1
CoPBA	$K_{0.05}Co[Co(CN)_6]_{0.66}\cdot 4.4H_2O$	1.9
FePBA(Co^{III})	$Fe[Co(CN)_6]_{2/3}\cdot 4H_2O$ (estimated)	2.5
CuPBA(Fe^{II}), $[Fe(CN)_6]$/Cu= 0.66	$K_{0.64}Cu[Fe(CN)_6]_{0.66}\cdot 3.2H_2O$	2.6
CuPBA(Fe^{II}), $[Fe(CN)_6]$/Cu= 0.59	$K_{0.33}Cu[Fe(CN)6]_{0.59}\cdot 4.1H_2O$	2.1
CuPBA(Fe^{II}), $[Fe(CN)_6]$/Cu= 0.57	$K_{0.19}Cu[Fe(CN)6]_{0.57}\cdot 4.4H_2O$	2.7
CuPBA	$K_{0.05}Cu[Fe(CN)_6]_{0.46}\cdot 5.0H_2O$	2.1
ion-exchange regin (IE)		0.38
zeolite 13X (ZL)		0.28
activated carbon (AC)		0.02

5. Crystal structure and morphology

The crystal structures of the samples were investigated using a powder X-ray diffractometer (PXRD, D8 Advance, Bruker Corp.) with Cu Kα radiation (λ=0.154 nm) at 40 kV and 40 mA, as shown in Fig. S6. Sample images were obtained using a field emission scanning electron microscope (FE-SEM, S-4800; Hitachi High Technologies Corp.) (Fig. S7). All measurements were taken at room temperature.

The estimated lattice size and crystallite sizes were 1.019 nm and 9.6 nm, respectively, for PB, 0.997 nm and 16.5 nm respectively for CuPBA, and 1.021 nm and 31.3 nm respectively for CoPBA.

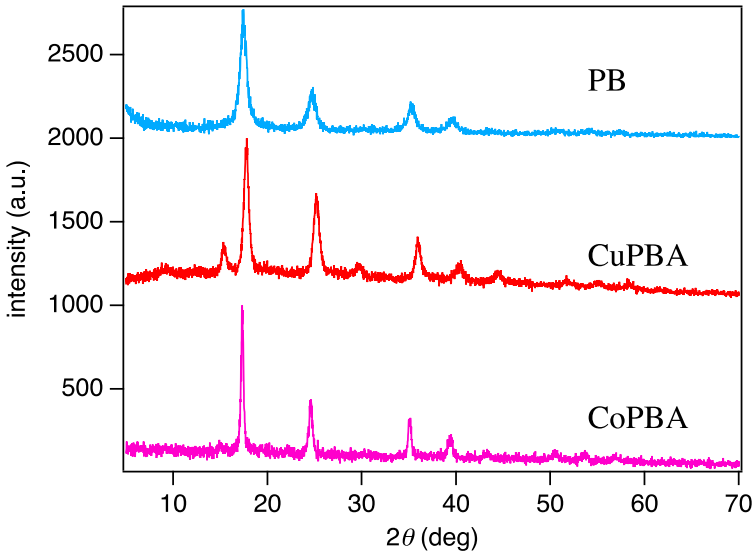

Figure S7. PXRD patterns of PB, CuPBA, CoPBA. The space group of crystal structure was Fm-3m.

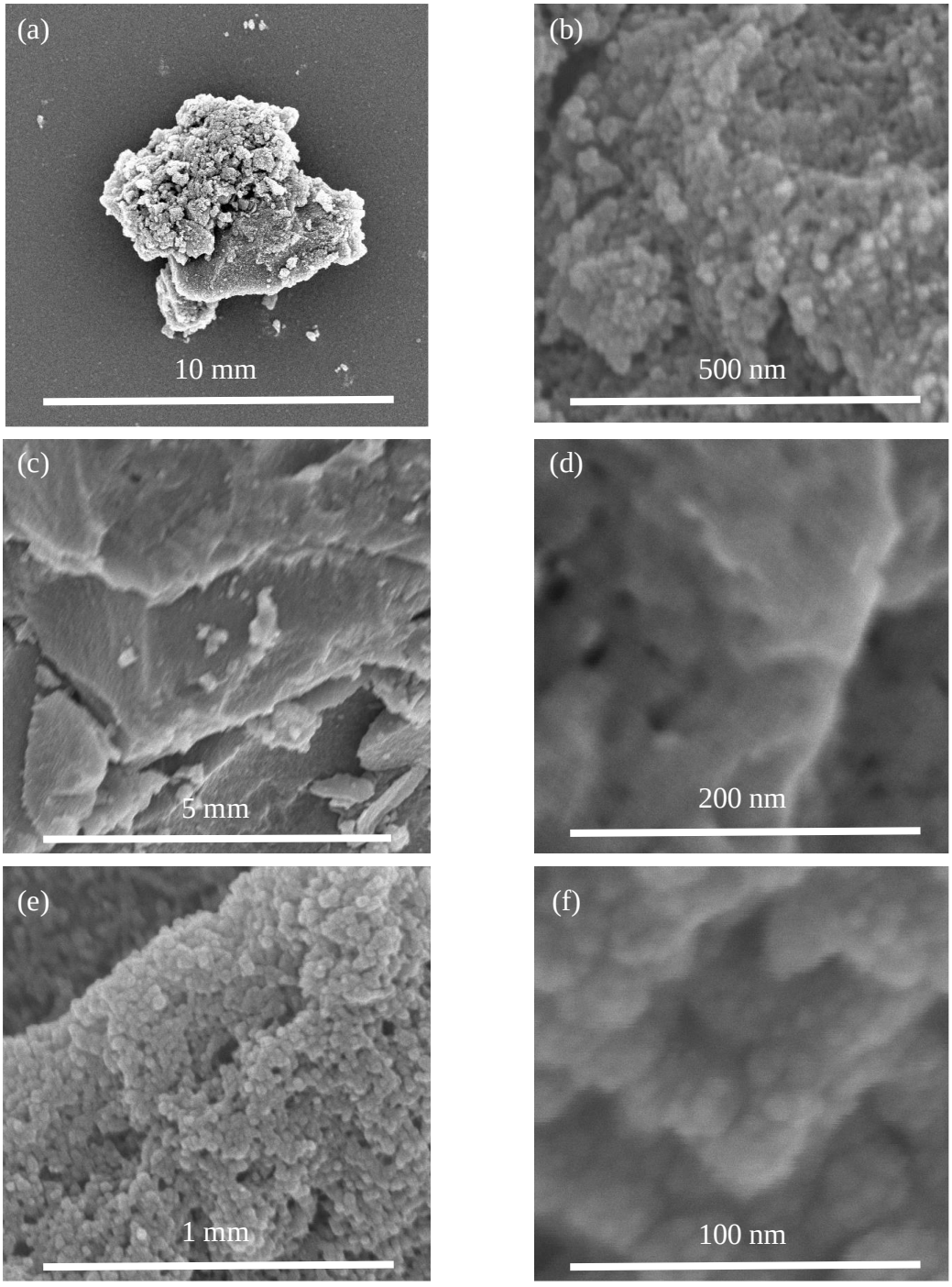

Figure S8. FE-SEM images of PB, CuPBA and CoPBA: (a) typical powder particle of PB, (b) primary particles of PB, (c) a typical powder particle of CuPBA, (d) primary particles of CuPBA, (e) typical powder particles of CoPBA, and (f) primary particles of CoPBA.

6. Specific surface area

Specific surface areas of samples were estimated using the Brunauer – Emmitt – Teller (BET) equation with N_2 adsorption isotherm at liquid nitrogen temperature (77 K). The nitrogen adsorption isotherms were obtained by using Belsorp-mini. The specific surface area was estimated with the following BET equation:

$$\frac{p}{(p-P_0)V_m} = \frac{C-1}{CV_m}\frac{p}{P_o} + \frac{1}{CV_m}$$

where p, p_0, C, and V_m respectively represent pressure, saturated vapor pressure, energy constant, and single molecular adsorption area. The so obtained nitrogen adsorption isothermic curves are presented in Fig. S8.

The estimated surface areas were 289 m^2 /g for PB, 675 m^2/g for CuPBA, and 862 m^2/g for CoPBA.

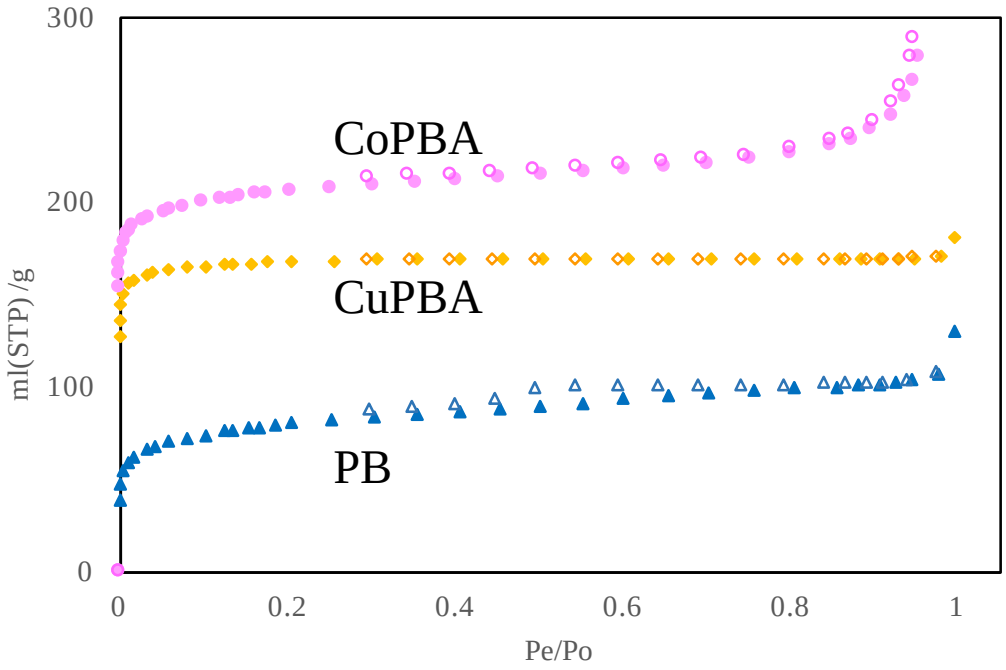

Figure S9. N_2 adsorption isothermic curves of PB, CuPBA, and CoPBA at 77 K.